

1 **Test beam results of a Cylindrical GEM detector for**  
2 **the BESIII experiment**

---

**G. Mezzadri<sup>b,i\*</sup>, M. Alexeev<sup>f</sup>, A. Amoroso<sup>f,l</sup>, R. Baldini Ferroli<sup>a,c</sup>, M. Bertani<sup>c</sup>,  
D. Bettoni<sup>b</sup>, F. Bianchi<sup>f,l</sup>, A. Calcaterra<sup>c</sup>, N. Canale<sup>b</sup>, M. Capodiferro<sup>c,e</sup>, V. Carassiti<sup>b</sup>,  
S. Cerioni<sup>c</sup>, JY. Chai<sup>a,f,h</sup>, S. Chiozzi<sup>b</sup>, G. Cibinetto<sup>b</sup>, F. Cossio<sup>f,h</sup>, A. Cotta  
Ramusino<sup>b</sup>, F. De Mori<sup>f,l</sup>, M. Destefanis<sup>f,l</sup>, J. Dong<sup>c</sup>, F. Evangelisti<sup>b</sup>, R. Farinelli<sup>b,i</sup>,  
L. Fava<sup>f</sup>, G. Felici<sup>c</sup>, E. Fioravanti<sup>b</sup>, I. Garzia<sup>b,i</sup>, M. Gatta<sup>c</sup>, M. Greco<sup>f,l</sup>, L. Lavezzi<sup>a,f</sup>,  
CY. Leng<sup>a,f,h</sup>, H. Li<sup>a,f</sup>, M. Maggiora<sup>f,l</sup>, R. Malaguti<sup>b</sup>, A. Mangoni<sup>d,k</sup>, S. Marcello<sup>f,l</sup>,  
M. Melchiorri<sup>b</sup>, M. Mignone<sup>f</sup>, G. Morello<sup>c</sup>, S. Pacetti<sup>d,k</sup>, P. Patteri<sup>c</sup>, J. Pellegrino<sup>f,l</sup>,  
A. Pelosi<sup>c,e</sup>, A. Rivetti<sup>f</sup>, M. D. Rolo<sup>f</sup>, M. Savrié<sup>b,i</sup>, M. Scodreggio<sup>b,i</sup>, E. Soldani<sup>c</sup>,  
S. Sosio<sup>f,l</sup>, S. Spataro<sup>f,l</sup>, E. Tskhadadze<sup>c,g</sup>, S. Verma<sup>i</sup>, R. Wheadon<sup>f</sup>, L. Yan<sup>f</sup>**

<sup>a</sup> *Institute of High Energy Physics, Beijing, China*

<sup>b</sup> *INFN, Sezione di Ferrara, Italy*

<sup>c</sup> *INFN, Laboratori Nazionali di Frascati, Italy*

<sup>d</sup> *INFN, Sezione di Perugia, Italy*

<sup>e</sup> *INFN, Sezione di Roma, Italy*

<sup>f</sup> *INFN, Sezione di Torino, Italy*

<sup>g</sup> *Joint Institute for Nuclear Research (JINR), Dubna, Russia*

<sup>h</sup> *Torino Politecnico, Italy*

<sup>i</sup> *University of Ferrara, Italy*

<sup>k</sup> *University of Perugia, Italy*

<sup>l</sup> *University of Torino, Italy*

*E-mail:* [gmezzadr@fe.infn.it](mailto:gmezzadr@fe.infn.it)

Gas detectors are very light instruments used in high energy physics to measure the particle properties: position and momentum. Through a high electric field it is possible to use the Gas Electron Multiplier (GEM) technology to detect the charged particles and to exploit their properties to construct a large area detector, such as the new IT for BESIII. The state of the art in the GEM production allows to create very large area GEM foils (up to  $50 \times 100 \text{ cm}^2$ ) and thanks to the small thickness of these foils it is possible to shape them to the desired form: a Cylindrical Gas Electron Multiplier (CGEM) is then proposed.

The innovative construction technique based on Rohacell, a PMI foam, will give solidity to cathode and anode with a very low impact on material budget. The entire detector is sustained by Permaglass rings glued at the edges. These rings are used to assemble the CGEM, together with a dedicated Vertical Insertion System and moreover they host the On-Detector electronics. The anode has been improved w.r.t. the state of the art through a jagged readout that minimizes the inter-strip capacitance.

The mechanical challenge of this detector requires a precision of the entire geometry within few hundreds of microns in the whole area. In this contribution an overview of the construction technique, the validation of this technique through the realization of a CGEM, and its first tests will be presented. These activities are performed within the framework of the BESIII/CGEM Project (645664), funded by the European Commission in the action H2020-RISE-MSCA-2014.

*5th International Conference on Micro-Pattern Gas Detectors (MPGD2017)  
22-26 May, 2017  
Philadelphia, USA*

---

\*Speaker.

### 3 1. Introduction

4 The possibility to employ gas detector, especially Micro Pattern Gas Detector, as tracking  
5 elements is well-exploited. Due to their lightness and robustness, Gas Electron Multipliers (GEMs)  
6 [1] are extremely favored for these types of applications.

7 BESIII will install a new Inner Tracker based on the Cylindrical GEMs in the summer of 2019.  
8 The CGEM-IT project is led by the Italian collaboration, but it involves Uppsala and Mainz Uni-  
9 versities, INFN and the Institute of High Energy Physics (IHEP) of Beijing. In order to show that  
10 the GEM technology can reach the experimental requirements, several test beams were performed.

### 11 2. BESIII and BEPCII

12 Beijing Spectrometer III (BESIII) is hosted at the Beijing Electron Positron Collider II (BEPC-  
13 II), at the IHEP. BEPC-II is a major upgrade of the preexisting accelerating structure. The beam en-  
14 ergy spans from 1 GeV to 2.3 GeV, allowing BESIII to collect data in the energy regime from 2 GeV  
15 to 4.6 GeV, which is frequently called  $\tau$  – *charm* regime. BESIII is a central symmetry detector  
16 optimized for flavor physics. A Main Drift Chamber (MDC), combined with the 1 T solenoidal  
17 magnetic field, currently allows to reconstruct the position and momentum of the charged particles.  
18 It is composed of two parts and the innermost layers can be extracted in case of radiation damage.  
19 Time-of-Flight (TOF) detectors allow to reconstruct the time of passage of particles, to start the  
20 identification process. A CsI(Tl) electromagnetic calorimeter (EMC) measures the energy of neu-  
21 tral and charged particles. Resistive Plate Chambers (RPCs) are placed in the return yoke of the  
22 magnet to operate as Muon Counters. A schematic view of the detector is shown in Fig. 1. The  
23 detector covers 93% of the  $4\pi$  solid angle and it is divided in two parts: the barrel ( $|\cos\theta| < 0.82$ )  
24 and the endcaps ( $0.86 < |\cos\theta| < 0.93$ ). More details on the BESIII detector can be found in  
25 Ref. [2].

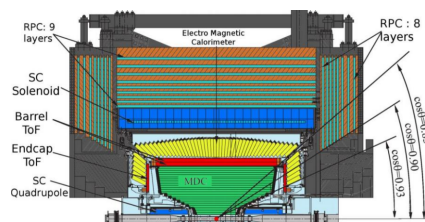


Figure 1: Schematic view of the BESIII detector.

#### 26 2.1 MDC Aging problems

27 The eight innermost layers of the MDC are showing aging effects: in order to prevent large  
28 discharges, that can compromise the detector operations, the first layers are operating with voltages  
29 lower than nominal ones, affecting the reconstruction efficiency. Since the BESIII data taking has  
30 been extended up to 2028 and in order to improve the performance a new Inner Tracker based on  
31 CGEM technology will be installed in summer 2019.

### 32 3. The CGEM-IT project

33 The CGEM-IT project will deploy a series of innovations and peculiarities in order to cope  
34 with the requirements provided by the BESIII collaboration, listed in Tab. 1.

Value	Requirements
$\sigma_{xy}$	$\leq 130 \mu\text{m}$
$\sigma_z$	$\leq 1 \text{ mm}$
dp/p @ 1 GeV/c	0.5%
Material Budget	$X_0 \leq 1.5\%$
Angular Coverage	93% of $4\pi$
Particle Rate	$\sim 10^4 \text{ Hz/cm}^2$
Minimum Radius	65.5 mm
Maximum Radius	180.7 mm

Table 1: List of the requirements provided by the BESIII collaboration for the new Inner Tracker

35 The CGEM-IT will consist of 3 layers of triple GEM detectors, shaped as cylinders. The  
36 mechanical rigidity is provided by gluing the GEM foils around moulds of fixed radii. Permaglass  
37 rings are used to operate as gas sealing structure and gap spacers. A sandwich of a PMI foam,  
38 called Rohacell, and kapton is used in order to provide mechanical rigidity to anode and cathode  
39 electrodes. Rohacell is a very light material that limits the material budget to  $0.3X_0$  per layer. A  
40 *jagged* anode is used to reduce the inter-strip capacitance up to 30% [3].

41 The most challenging requirement for the CGEM-IT development is the spatial resolution of  
42  $\sigma_{xy} < 130 \mu\text{m}$  in 1 Tesla magnetic field. A dedicated ASIC is being developed to provide time  
43 and charge information for each strip. In order to assess that the CGEM-IT can reach the required  
44 performance an extensive series of test beams was performed in the last few years within the test  
45 beam activities of the RD51 Collaboration of CERN.

### 46 4. Test Beam results

47 The tests were performed both on  $10 \times 10 \text{ cm}^2$  planar GEM chambers and on a cylindrical  
48 prototype of the dimension of the second layer of the final CGEM-IT. All the tests were performed  
49 in H4 line of the SPS, in CERN North Area. Since the CGEM-IT will operate in a magnetic field,  
50 all the test chambers were placed inside Goliath, a dipole magnet that can reach up to 1.5 T in both  
51 polarities. Pion and muon beams were used: the momentum of the beam is 150 GeV/c. Scintillators  
52 were placed upstream and downstream the magnet to operate as trigger. The typical used setup is  
53 sketched in Fig. 2, where the setup with the cylindrical prototype is shown.

#### 54 4.1 Position reconstruction with Charge Centroid

55 The Charge Centroid (CC) readout uses of the charge induced on each strip to reconstruct the  
56 position where the particle passed. The  $x_{CC}$  is defined has followed:

$$x_{CC} = \frac{\sum_i x_i q_i}{\sum_i q_i} \quad (4.1)$$

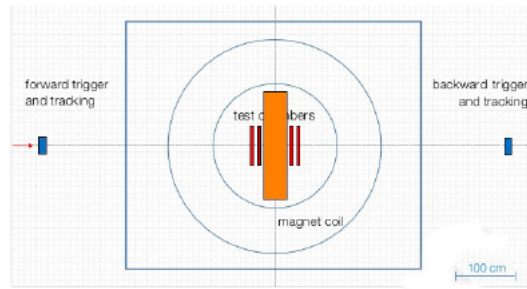


Figure 2: Sketch of the setup for the test beams. Here is the one used for the cylinder, but the one with planar chambers have similar features.

57 where  $x_i$  is the  $i$ -th strip coordinate and  $q_i$  is the charge induced on the  $i$ -th strip. If the  
 58 avalanche has a Gaussian shape at the anode, the CC works properly and improves the best achiev-  
 59 able digital readout resolution, that is of the order of  $p/\sqrt{12}$ , where  $p$  is the strip pitch ( $p = 650\ \mu\text{m}$ ).

#### 60 4.1.1 Results with no magnetic field applied

61 We tested planar and cylindrical GEMs spatial resolution and efficiency with no magnetic field  
 62 applied.

63 **Planar GEMs** The analysis of the data shows that an efficiency plateau can be reached starting  
 64 from total gains of about 5000 with a typical value around 98%. In Fig. 3 the resolution with  
 65 respect to the mean cluster size is plotted. It is possible to clearly notice that a spatial resolution  
 66 below  $100\ \mu\text{m}$  can be achieved for very different cluster sizes. An extensive collection of results  
 67 for planar GEMs with no magnetic field can be found in Refs. [4, 5].

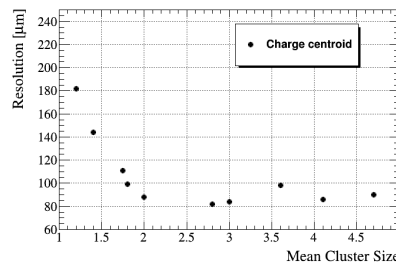


Figure 3: Spatial resolution with respect to the cluster size.

68 **Cylindrical prototype** We have tested a cylindrical prototype. In order to simplify the recon-  
 69 struction, only the  $\phi$  view was instrumented. The goals were to test the construction procedure and  
 70 to have a first comparison between a cylindrical and a planar GEM.

71 The cluster size and the spatial resolution are investigated as a function of the cluster charge.  
 72 The resolution is measured as the width of the distribution of the differences between the recon-  
 73 structed position of the front and the back of the cylinder. Fig. 4a and Fig. 4b show the summary  
 74 plots for cluster size and resolution respectively.

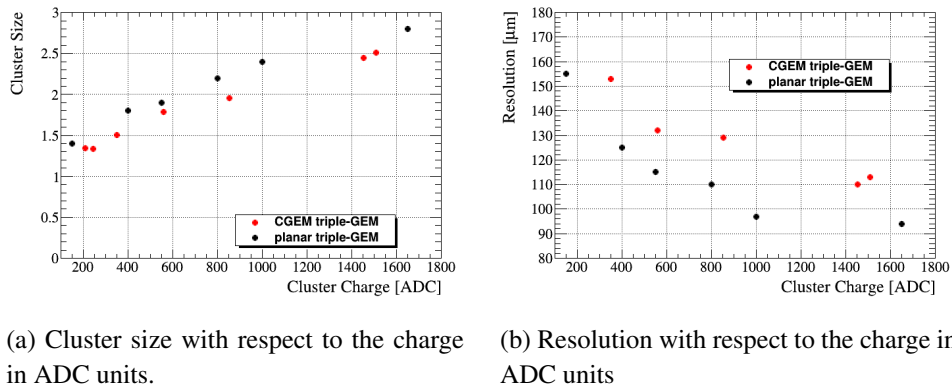


Figure 4: Study of the performance of planar (red circles) and cylindrical (black circles) prototypes.

75 CGEM provide similar response to the planar GEMs. Further investigations are on-going in  
 76 order to deeply understand the CGEM performance.

77 **4.1.2 Results with magnetic field**

78 Planar GEMs performance in magnetic field was studied. The presence of an external magnetic  
 79 field induces a deformation of the avalanche shape at the anode due to the Lorentz force: the charge  
 80 centroid method performance degrades almost linearly with the magnetic field as shown in Fig. 5a.

81 It is still possible improve the performance by a proper optimization of the drift field as shown  
 82 in Fig. 5b. With the proper choice of gas mixture (Ar/iC<sub>4</sub>H<sub>10</sub> (90/10)) and drift field (2.5 kV/cm)  
 83 is possible to achieve the unprecedented resolution of  $\sigma_x$  190  $\mu$ m in 1 Tesla magnetic field.

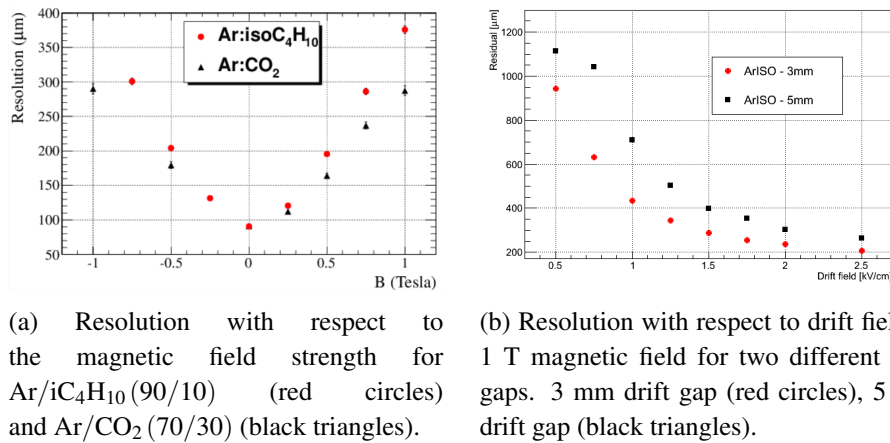


Figure 5: Studies of the resolution in presence of a magnetic field.

84 **4.1.3 Combination of non-orthogonal incident tracks and magnetic field**

85 In the final BESIII environment, the CGEM-IT will have to reconstruct tracks with very dif-  
 86 ferent incident angles in 1 Tesla magnetic field. Fig. 6 shows the possible combinations of effects.  
 87 Two angles appear, one due to the Lorentz force ( $\alpha_{Lorentz}$ ) and the other due to the non-orthogonal

88 incident angle ( $\alpha_{track}$ ). Different combinations of the two angles produce different charge shapes  
 89 at the anode, and thus the resolution of CC degrades or improves accordingly. The CC gives the  
 90 best performance when  $\alpha_{Lorentz} \sim \alpha_{tracks}$  (right plot on the sketch)

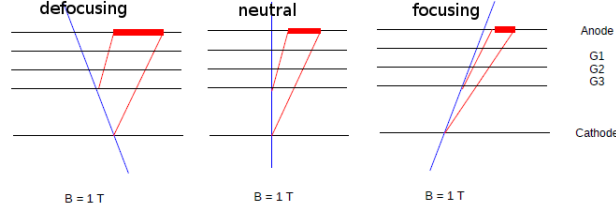


Figure 6: Effects of the combination of magnetic field and incident tracks angles. (Left)  $\alpha_{Lorentz} \neq \alpha_{track}$ ,  $\alpha_{track} \neq 0$ , defocusing. (Center)  $\alpha_{Lorentz} \neq \alpha_{track}$ ,  $\alpha_{track} = 0$ , standard. (Right)  $\alpha_{Lorentz} \sim \alpha_{track}$ , focusing.

## 91 4.2 Position reconstruction with $\mu$ TPC readout

92  $\mu$ TPC readout is an innovative method that exploits the few millimeters drift gap as Time  
 93 Projection Chamber. Indeed, the time of arrival of the induced charge on the strip can be used to  
 94 reconstruct the first ionization position in the drift gap and thus improve the spatial resolution. To  
 95 fully operate in  $\mu$ TPC mode, it is necessary to know both the drift velocity and the time of arrival of  
 96 the induced signals. The latter is extracted from the electronics, while the former can be extracted  
 97 from Garfield simulations.

98 Once the different first ionization positions are reconstructed in the drift gap, it is possible to  
 99 compute the track position by means of a linear fit to the found bidimensional points. The position  
 100 is extracted by the following equation:

$$x_{\mu TPC} = \frac{\frac{gap}{2} - b}{a} \quad (4.2)$$

101 where  $a$  and  $b$  are the straight line parameters and  $gap$  is the drift gap thickness. This innova-  
 102 tive readout was firstly developed for ATLAS MicroMEGAS [6]. This is the first application of the  
 103 method to GEMs in magnetic field. All the following results are extracted only from planar GEMs.

### 104 4.2.1 Results with non-orthogonal tracks in 1 T magnetic field

105 The presence of the magnetic field produces an interplay between the Lorentz angle and the  
 106 incident angle to determine the final shape of the avalanche, and thus, to the performance of the  
 107  $\mu$ TPC readout. The Lorentz angle is determined by the gas mixture, the drift fields and the ex-  
 108 ternal magnetic field applied, while the incident tracks angle is varied by rotating the chambers.  
 109 Fig. 7 shows the spatial resolution with respect to the track incident angle for Ar/CO<sub>2</sub> (70/30) gas  
 110 mixture, with 1.5 kV/cm drift field and 1 Tesla magnetic field with respect to the incident track  
 111 angle. The red circles and the black triangles represent the planar and the cylindrical prototype  
 112 respectively.

113 A spatial resolution better than 200  $\mu$ m has been achieved for a very wide set of incident angles  
 114 with the  $\mu$ TPC mode. The focusing effect is already present at 10°, but has maximum impact when

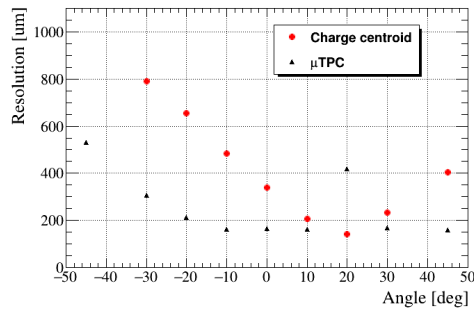


Figure 7: Resolution with respect to the incident angle of the track in 1 Tesla magnetic field.

115  $\alpha_{track} \sim \alpha_{Lorentz} \simeq 20^\circ$ . Here it affects the result for the  $\mu$ TPC, but, as expected, the charge  
 116 centroid method has its best resolution. A merge of the two techniques will combine the  $\mu$ TPC and  
 117 CC information in order to achieve a better resolution and match the BESIII requirements.

## 118 5. Final remarks

119 A series of test beams has been performed to validate the cylindrical GEM technology and to  
 120 address its limits in terms of spatial resolution in high magnetic field.

121 The first test beam with the cylindrical GEM shows that the CGEM technology can operate  
 122 in beam condition with performance similar to the planar one. More indications will come from  
 123 the analysis of the data from the test beam performed in July 2017, with the actual layer 1 (the  
 124 innermost in the final BESIII CGEM-IT) and from extensive cosmic rays data taking.

125 In order to satisfy the spatial resolution requirement, two readout modes are deployed. With  
 126 the conventional Charge Centroid method it is possible to achieve the unprecedented resolution of  
 127  $\sigma_x \sim 190 \mu\text{m}$  with orthogonal tracks in magnetic field. The  $\mu$ -TPC readout mode improves and  
 128 overcomes the charge centroid limits granting a spatial resolution lower than  $200 \mu\text{m}$  for a large  
 129 angle interval. These results represent the world best results for GEM in magnetic field. By a  
 130 merge of the two readout modes will be possible to satisfy the BESIII requirements.

## 131 References

- 132 [1] F. Sauli, Nucl. Instr. and Meth. A **386** (1997) 531-534.  
 133 [2] BESIII Collaboration, Nucl. Instr. Meth. A **598** (2009) 7-1100000  
 134 [3] D. Bettoni *et al.*, PoS(TIPP2014) 292 (2014)  
 135 [4] G. Mezzadri, J. Phys. Conf. Ser. **742**, no.1, 012036 (2016)  
 136 [5] A. Amoroso *et al.* Nucl. Instrum. Meth, A **824**, 515 (2016)  
 137 [6] T. Alexopoulos *et al.*, Nucl. Instrum. Meth. A **617** (2010) 161.